ELSEVIER

International Journal of Mass Spectrometry 182/183 (1999) 261–273

International Journal of Mass Spectrometry

Differentially heated capillary for thermal dissociation of noncovalently bound complexes produced by electrospray ionization

Fei He, Javier Ramirez, Benjamin A. Garcia, Carlito B. Lebrilla*

Department of Chemistry, University of California, Davis, CA 95616, USA

Received 6 August 1998; accepted 2 November 1998

Abstract

A heated capillary consisting of two independently heated segments is used to dissociate gas-phase complexes of peptides and β-cyclodextrin. By fixing the temperature in the first segment and varying it in the second segment, the complex is first desolvated and then dissociated. The results indicate that the complex is dissociated in the gas phase rather than in the solution phase of an intact droplet. The thermal dissociation profile, the dissociation temperature and apparent Arrhenius parameters E_a and A are obtained. These values are compared to E_a obtained from blackbody infrared radiation dissociation. (Int J Mass Spectrom 182/183 (1999) 261–273) © 1999 Elsevier Science B.V.

Keywords: Differentially heated capillary; Noncovalently bound complex; Cyclodextrin; Peptide

1. Introduction

The relatively small amounts of internal energy deposited in the ion during ionization makes electrospray ionization (ESI) mass spectrometry an ideal method for characterizing noncovalently bound complexes generated from solution. There are several examples of gas-phase complex formation by ESI MS [1–11], however characterizing the nature of the interaction remains a difficult task. Dissociation methods such as collision-induced dissociation, photodissociation, surface-induced dissociation, and others that are typically used for molecular or quasimolecular ions often do not work efficiently or are not sufficiently characteristic for noncovalently bound complexes. A method that shows considerable promise employs a heated capillary found in some designs of ESI sources [12]. Smith and co-workers utilized a single heated stage metal capillary to obtain activation energies of multiply charged ions of melittin produced by electrospray [13,14]. These authors report that the apparent activation energies decrease with increasing charge states from + 3 to + 6. Wysocki and co-workers also reported a thermal decomposition method using a heated capillary to dissociate the protonated monomer and dimer of leucine enkephalin [15]. We extended this method to noncovalent complexes, most notably complexes of protonated peptides and β cyclodextrin. We re-

* Corresponding author.

Dedicated to the memory of Ben Freiser to commemorate his many seminal contributions to mass spectrometry and gas phase ion chemistry.

PII S1387-3806(98)14258-6

ported the use of heated capillary dissociation (HCD) as a simple and fast method for determining the relative order of gas-phase stability [16]. We showed further that complexes can be dissociated as the temperature of the capillary is raised until a specific temperature is reached (the dissociation temperature) where the complex is no longer observed. The dissociation temperatures of the complexes were compared to threshold collision-induced dissociation (CID) results and a direct correlation in the results of the two dissociation methods was found. However, in the previous report we could not determine whether the dissociation of the complex was a solution-phase or a gas-phase event. In other words, does the complex dissociate in the droplets that are known to exist in the spray before they become gas-phase ions, or is the complex desolvated in the gas-phase and dissociated as a gas-phase species? To answer these questions, a new differentially heated capillary was designed and constructed. The first segment is used to desolvate the complex while the second segment is used to dissociate the complex.

Complexes of cyclodextrins in solution are believed to involve noncovalent interactions. They have long been studied in solution [17–23] but have recently been of interest in mass spectrometry [24–26]. Cyclodextrins are cyclic oligosaccharides consisting of glucopyranose subunits. The most common cyclodextrins are α, β, and γ cyclodextrin, composed of six, seven, and eight glucose units, respectively. The glucose units are α–1-4 linked, forming a truncated conical structure with a narrower and a wider rim. The wider rim is composed of the two and three hydroxyl groups of the glucose while the narrower rim is composed of the six hydroxyl groups. The hydroxyl positions are sometimes alkyl derivatized to give the compound greater solubility [27]. The rim is hydrophilic while the outer surface and the inner cavity are hydrophobic. In solution, organic compounds, particularly phenyl rings, are known to include into the cyclodextrin cavity [28]. There remains a controversy whether the gas-phase complexes retain the inclusion structure characteristic of the solution-phase species [24–26].

In this paper we report the design and characterization of the newly designed differentially heated capillary. This arrangement allows two segments to be independently heated. Results of heated capillary dissociation (HCD) of cyclodextrin–peptide complexes using this new design are shown and compared with results from blackbody infrared radiation dissociation (BIRD) [29] obtained earlier in this laboratory [30].

2. Experimental

Bradykinin (BK, RPPGFSPFR), and three of its analogs: lysine^1-bradykinin (L^1-BK, KPPGFSPFR), desArg^1-bradykinin (dR^1-BK, PPGFSPFR), desArg^9-bradykinin (dR^9-BK, RPPGFSPF) and heptakis-tri-O-methyl-β-cyclodextrin (β-CD) were obtained from Sigma Chemical Co. (St. Louis, MO) in the highest purity and used without further purification. The electrospray solutions were prepared by dissolving 2:1 molar ratio of peptide and cyclodextrin in 50:50 water:methanol solvent to yield a β-CD concentration of 2.0×10^{-5} M.

The experiments were carried out using a home-built electrospray Fourier transform mass spectrometry (FTMS) equipped with an Oxford (Oxford Instruments, Witney, England) 5-tesla superconducting magnet. Description of the instrument and its capabilities are provided in earlier publications [31,32]. The analyte solution was transported from the syringe pump to the electrospray needle via a 50 mm fused silica tubing. The solution flow rate was maintained at 8 mL/min in all experiments. The charged droplets produced by the 3 kV electrospray needle, whose tip is approximately 5 mm from the counter electrode (capillary), drift down-field toward the front end of the capillary. Gas-phase ions were produced by completely desolvating the droplets in the capillary. Ions travel through a single stage quadrupole into a 2 inch cubic analyzer cell. The ions are translationally cooled by two pulses of N_2 gas which increase the pressure to 10^{-5} Torr momentarily.

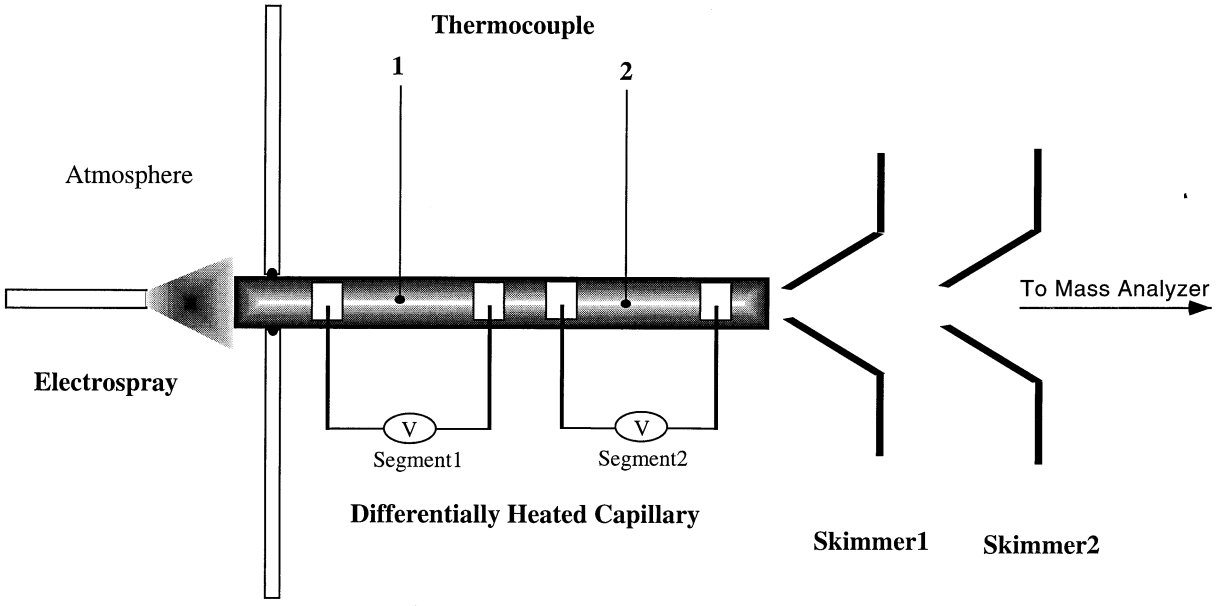

Scheme 1.

2.1. Apparatus

The capillary is mounted inside a home-built electrospray source. The solvated ions produced from the electrospray needle travel through the heated capillary and a set of skimmers and lenses (Scheme 1). Only the relevant features of the newly designed capillary will be described here. The capillary is made of stainless steel with 1.9 mm o.d., 0.5 mm i.d., and 28 cm length. The capillary is divided into two independently heated segments of equal length (12 cm), with the one close to the electrospray needle (front end) designated Segment1, and the one close to the ion cyclotron resonance (ICR) cell (back end) designated Segment2. The total heated length is 24 cm with about 4 cm unheated and extends from Segment1 to atmosphere at the entrance of the vacuum chamber. The lengths of the individual segments are smaller than that used by Wysocki and by Smith. The intensities of the complexes are not as great as that of the peptides studied by the previous researchers, and there was some concern that the ion intensity of the complexes would decrease too severely for the signal to be observed in a longer capillary. Wysocki used both an 18 cm and a 30 cm capillary. They found that increasing the length to 30 cm does not vary the results significantly. In that report, the authors also used two capillaries: an external segment located outside the vacuum chamber, and an internal segment located in the vacuum chamber. However, only the temperature of the external capillary was varied.

Both capillary segments are resistively heated by two independent dc power supplies. Contact is made with machined copper blocks that clamp on to the capillary and soldered to power supply lines. Each segment has a *J* type thermocouple spot welded to the middle of the segment where the temperature is monitored throughout the whole experiment. Because of the dynamic nature of the system, a temperature gradient exists in the capillary. The temperature is measured in the middle of each segment, where it is the highest for the segment.

3. Results

3.1. HCD of cyclodextrin bradykinin complex

The temperature characteristics of one segment as the other is heated are shown in Fig. 1. Fig. 1(a) shows the temperature response of Segment1 when

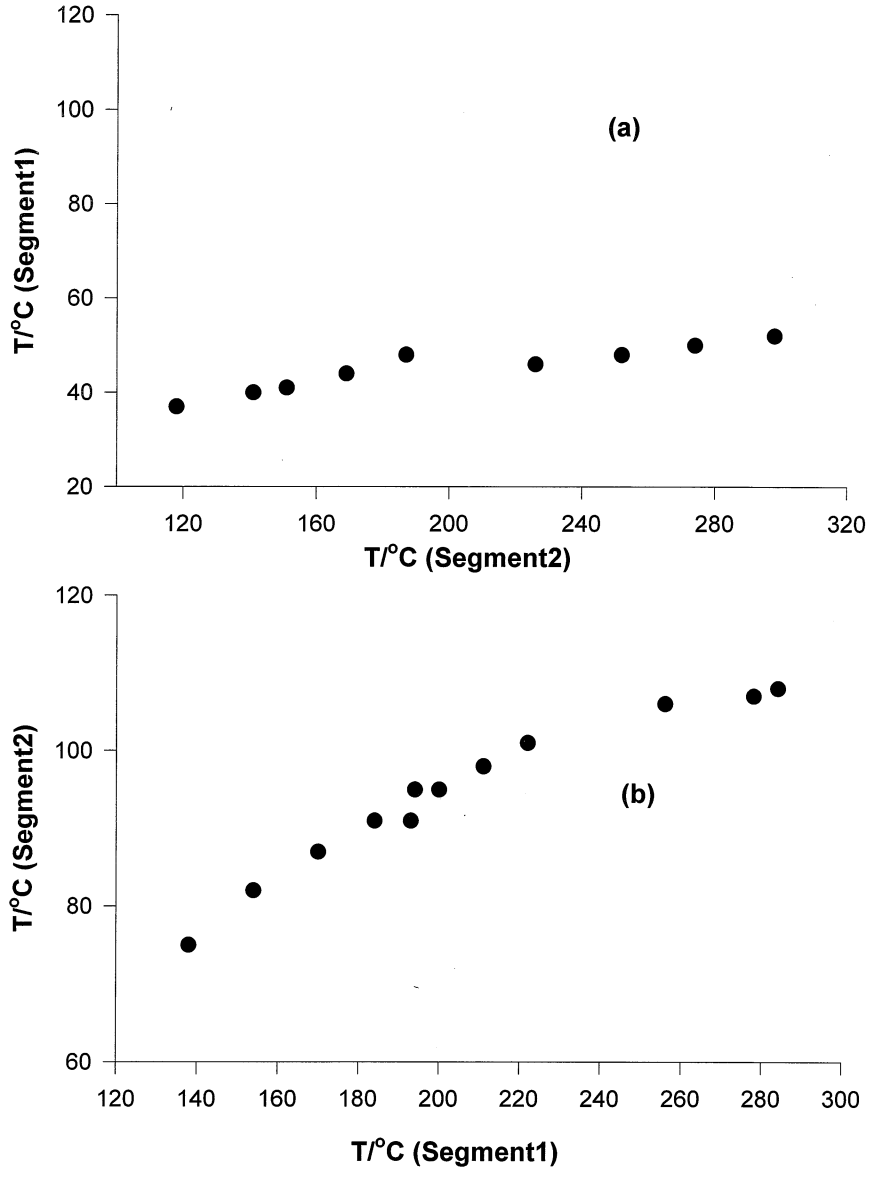

Fig. 1. The temperature measured on Segment1 when Segment2 (a) is heated and vice-versa (b).

Segment2 is heated. Varying the temperature of Segment2 from 120–300 °C, changed the temperature of Segment1 from about 30–50 °C. Segment1 is opened directly to atmosphere, however a minor heat transfer still occurs from Segment2 to Segment1 when the former is heated even in the presence of a large material flow in the opposite direction. When the temperature of Segment1 is increased from 130–300 °C, the temperature of Segment2 rose similarly from about 70–110 °C (Fig. 1(b)). That the temperature in Segment2, which is downstream of Segment1, is not even higher is because of several factors including the relatively poor thermal transfer between the interior and exterior of the capillary—stainless steel has poor thermal conducting properties—and the large flow of ambient air into the capillary.

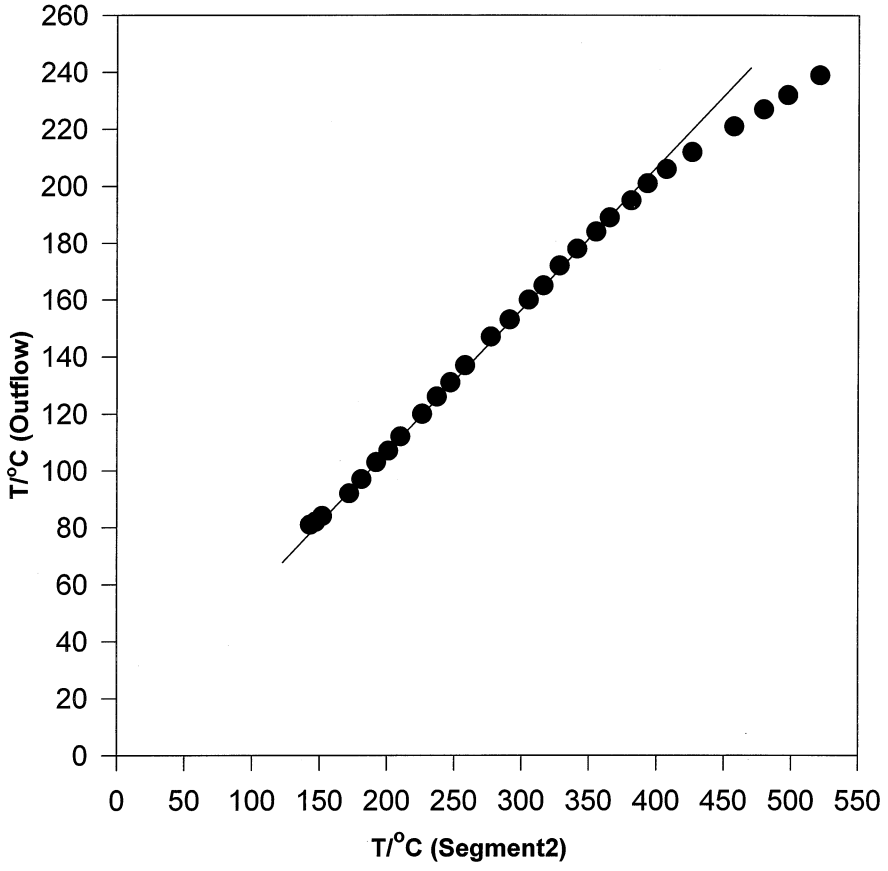

Fig. 2. The temperature of the outflow vs the temperature on Segment2 with the thermocouple placed 1 mm from the capillary exit.

Attempts were made to monitor the temperature of the gas by placing a thermocouple gauge directly behind (~ 1 mm) the capillary. This produced the plot shown in Fig. 2. The expansion of the gas, though minimal (from 100–1 Torr), may contribute to the temperature difference between the outflow and Segment2. However, it appears that the internal temperature is about half of that monitored externally. More importantly, the response is not linear. At higher temperatures (> 400 external temperature), the increase in the interior temperature becomes smaller.

Fig. 3(a) shows the intensities of the complex peak $[CD:BK + H]^{+2}$, normalized to the sum of all intensities in the spectrum, at different temperatures of Segment1. No heat is applied to Segment2. At low temperatures, the complex peak intensity increases with increasing temperature. At this temperature range, desolvation occurs. At about 180 °C, the curve levels off until 260 °C. Unless otherwise stated, all temperatures cited will henceforth correspond to the exterior temperature of the capillary. In this "stable" region, we suspect that desolvation is complete and the complex is further heated without undergoing dissociation. This region may correspond to a gas-phase rearrangement where the complex converts from the "solution-phase" structure to a "gas-phase" structure. In solution phase, formation of the inclusion complex may be the driving force for interaction, whereas in the gas phase the complex is maintained by ion-dipole interactions involving the protonated sites on the peptides and the hydrophilic rim of the cyclodextrin.

When the temperature of Segment1 is increased above 260 °C, the intensity of the complex decreases.

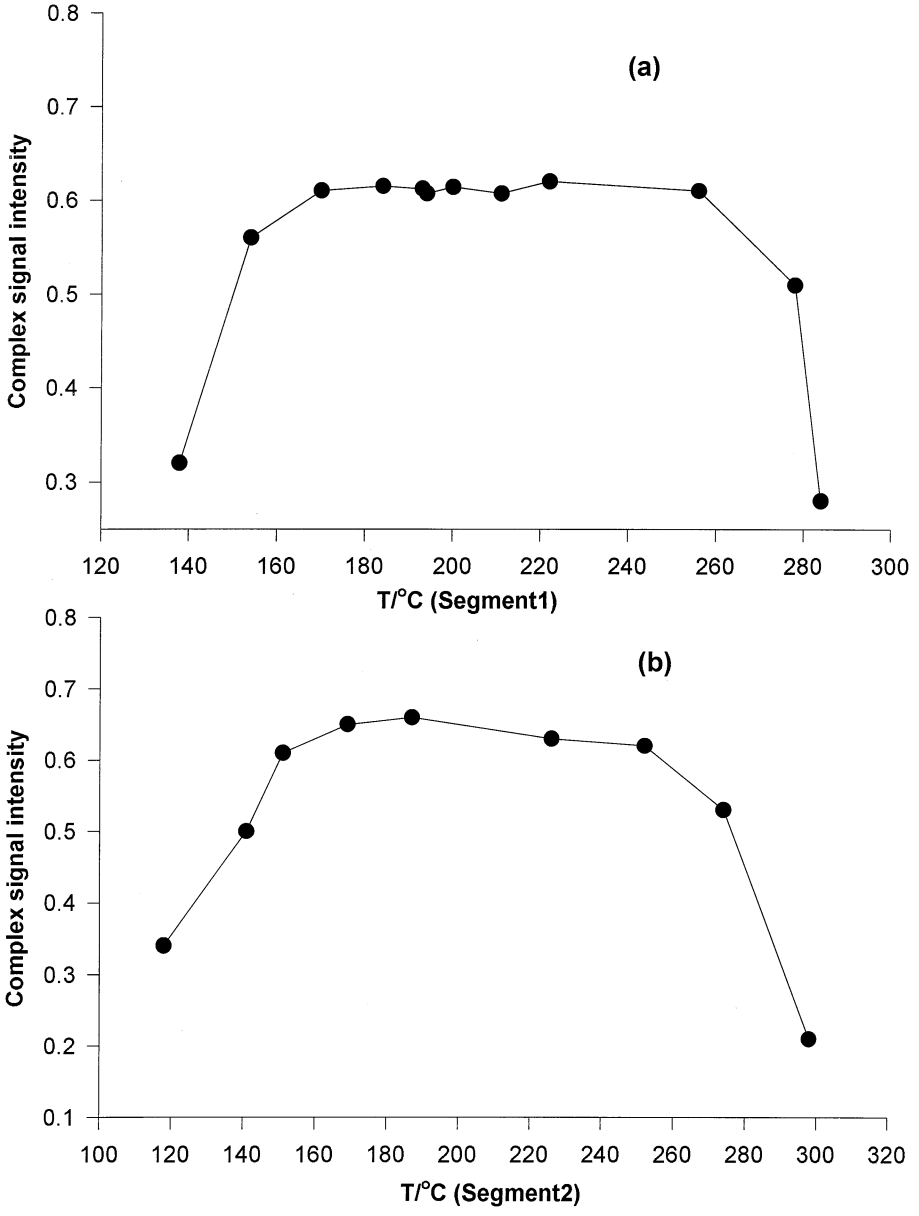

Fig. 3. (a) The intensities of the complex peak [CD: BK + H]$^{2+}$ (normalized to the sum of all intensities) at various temperatures of Segment1 with no heat applied to Segment2. (b) The same experiment with Segment2 heated.

At this point the complex dissociates and the corresponding intensity decreases until the signal is no longer observed. Similar behavior is obtained in the analogous experiment where Segment2 is heated (Fig. 3(b)).

To ensure that the dissociation is occurring in the gas-phase rather than solution phase, the HCD experiments were performed by setting the temperature of Segment1 to some value in the stable region, while the temperature on Segment2 is increased. At least two scenarios for complex dissociation are proposed. The complex may either dissociate in the droplet and

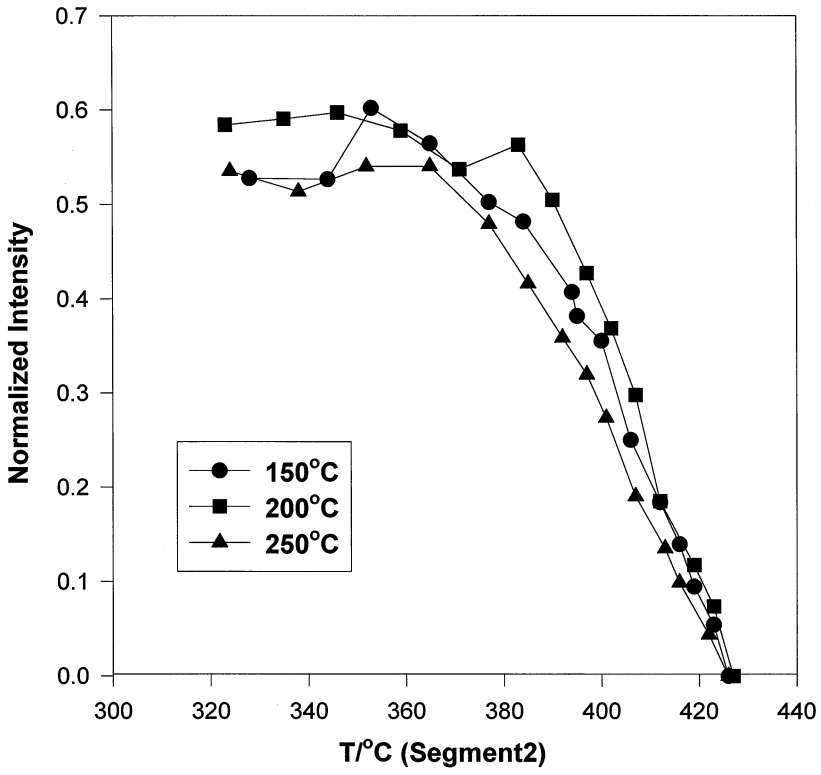

Fig. 4. The dissociation behavior of the complex [CD: BK + H]$^{2+}$ with Segment1 fixed to 150, 200, and 250 °C and Segment2 varied.

desolvate, or it may desolvate first and then dissociate. The latter is the desired gas-phase process. For each complex, the dissociation profile such as that shown in Fig. 3 is determined to establish the temperature where Segment1 should be set. During the experiments, all other conditions including electrospray needle voltage, capillary voltage, lens and skimmer voltages are held constant unless specified. The Segment2 temperature is monitored until the complex peak intensity is below 1% of the most abundant peak. This temperature is called the dissociation temperature or T_d (vida supra).

By plotting intensity of the complex (normalized to all intensities) as a function of the temperature on Segment2, HCD plots are obtained. The dissociation behavior of the bradykinin complex [CD:BK + 2H]$^{2+}$ is shown in Fig. 4. Fixing the temperature of Segment1 to an area in the stable region as in Fig. 3 and varying the temperature on Segment2 shows that indeed the dissociation is a gas-phase process rather than one occurring in the droplet. The intensity of the complex varies strongly with the temperature of Segment2. The temperatures on Segment1 set at three different temperatures (150, 200 and 250 °C) illustrate similar dissociative behavior. More importantly, nearly identical dissociation temperatures (T_d) of [CD:BK + 2H]$^{2+}$ on Segment2 were obtained for three temperatures of Segment1 (Fig. 4).

A typical spectrum for [CD:BK + 2H]$^{2+}$ obtained in the stable region (T = 200 K for both segments) is shown in Fig. 5(a). Under these conditions, the intensity of the complex is about 50% of the base peak. Also observed are signals corresponding to ammoniated, sodiated and potasiated cyclodextrin. For comparison the mass spectrum at a point near the dissociation temperature is shown in Fig. 5(b). The temperature on Segment1 was set to 200 °C, which corresponds to the middle of the stable region. The temperature on Segment2 was 418 °C, which was close to T_d and the complete dissociation of the

Table 1

	$[CD:BK + 2H]^{2+}$	$[CD:L^1\text{-}BK + 2H]^{2+}$	$[CD:dR^1\text{-}BK + 2H]^{2+}$	$[CD:dR^9\text{-}BK + 2H]^{2+}$
E_a(HCD), eV	2.65	2.49	2.22	2.16
E_a(BIRD), eV	1.07	0.98	0.72	0.64
ΔE_a	1.58	1.51	1.50	1.52
log A(HCD)	25.5	24.7	21	22.4
log A(BIRD)	11.4	10.0	6.2	7.8
Δlog A	14.2	14.7	14.8	14.6
T_d, °C	426	425	457	360
E_{com}, eV	1.2	1.2	1.5	1.0

$[CD:BK + 2H]^{2+}$ complex. Ions are observed corresponding to the fragmentation of the peptide. The fragments are labeled according to the types of cleavages that produce them. No fragments of the cyclodextrin are observed. These results contrasts to BIRD experiments where some fragments of the peptides remain associated with cyclodextrin [30]. The source of the fragment, whether from the complex or the free peptide is not immediately evident. That peptide fragmentation is observed even in the presence of some abundance of complex indicate that the interactions in the complex are strong. The sum of the intermolecular forces that retain the complex are evidently as strong as the covalent bonds in the peptide. We reported similar conclusions in the BIRD experiments [30].

The T_d of four peptide complexes are tabulated in Table 1. CID threshold energies previously obtained in this laboratory are also listed for comparison. CID is a more established method to study gas-phase dissociation energy. Table 1 clearly shows that the relative order of HCD and CID agree well with each other.

3.2. Determination of apparent dissociation energy E_a(HCD) and the apparent preexponential factor A(HCD)

The dissociation reaction the complex undergoes as it travels through the capillary is represented by

$$[CD: P + 2H]^{+2} \rightarrow \text{Products}$$

where CD is β cyclodextrin and P is the peptide. The lack of mass selection before the heated capillary makes it difficult to specifically assign the products. For a unimolecular dissociation, the rate of dissociation can be written as:

$$kt = \ln (I_o/I) \tag{1}$$

where k is the rate constant for the first order reaction, t is the time the ions traverse the capillary, I_o is the initial intensity of the complex, and I is the intensity of complex at a fixed temperature. The value I_o was determined by the intensities at the stable region. Both I and I_o are normalized to an internal reference, which is chosen to be the sodiated cyclodextrin peak. This species is generally unreactive in the temperature range of the experiments. Inserting Eq. (1) into the Arrhenius Eq. (2)

$$\ln k = \ln A - (E_a/RT) \tag{2}$$

yields

$$\ln \left[\ln \left(\frac{I_o}{I} \right) \right] = \ln A - \frac{E_a}{RT} \tag{3}$$

By plotting ln [ln (I_o/I)] versus $1/T$, a slope equal to E_a/R is obtained as well as an intercept equal to ln A + ln t. Because of uncertainties in the measurements of T and the complexity of the dissociation processes, the values obtained are apparent and are designated as E_a(HCD) and A(HCD), respectively.

The residence time (t) of the ion in the capillary tube was estimated. Under experimental conditions, the Reynold's number was determined and is found to correspond to laminar flow [33]. The flow rate for gas inside a tube was calculated by Poiseuille's formula

$$\frac{dV}{dt} = \frac{(P_1^2 - P_2^2)\pi r4}{161 \eta P_o} \tag{4}$$

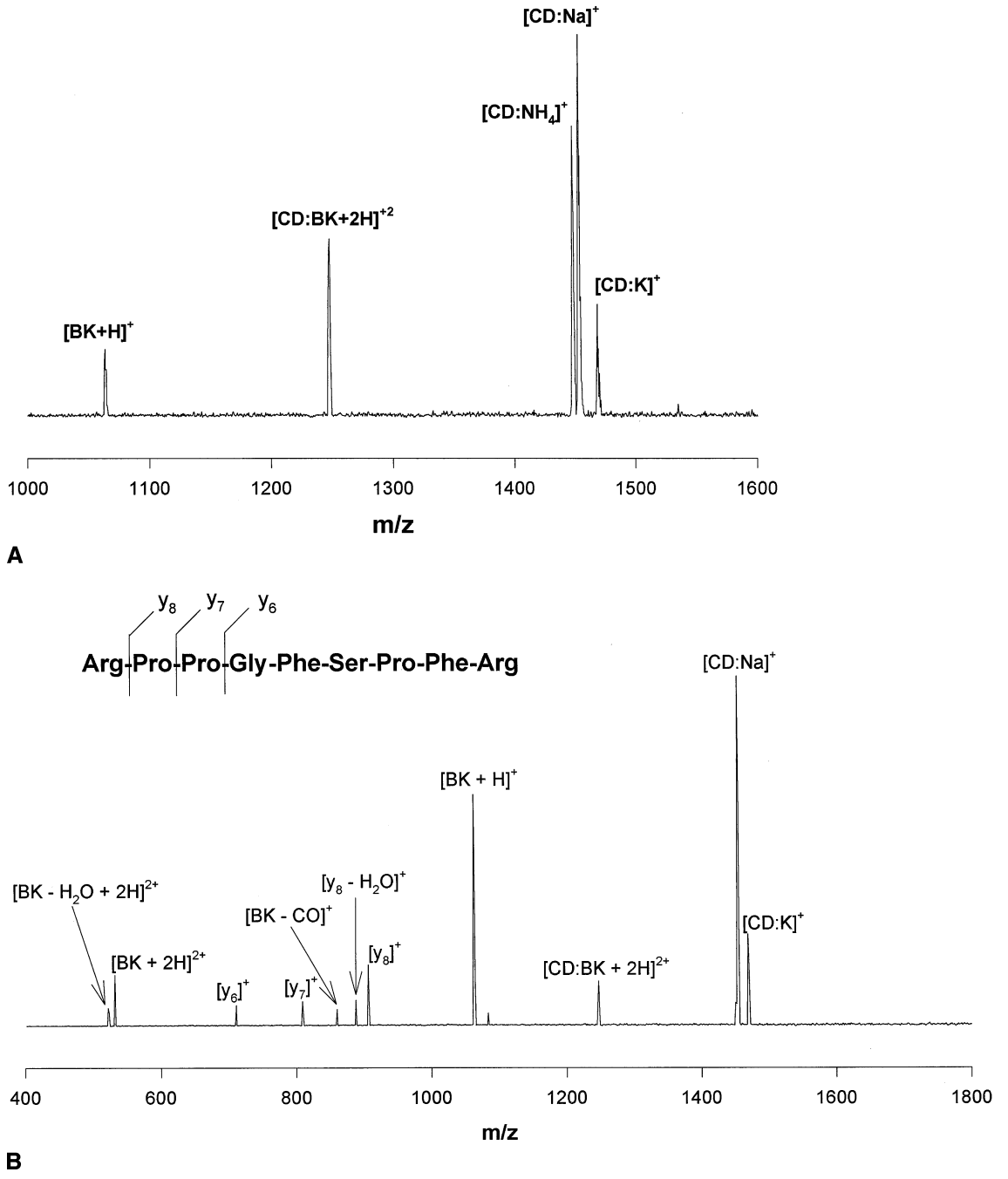

Fig. 5. The FTMS spectra of the complex [CD: BK + H]$^{2+}$ with Segment1 set to 200 °C and Segment2 set to (a) 200 °C and (b) 418 °C.

where V is the flow volume, t the time, P_1 and P_2 the pressures at two ends of the tube, P_o the reference pressure (chosen as P_2), η the coefficient of viscosity, l and r the length and radius of the tube, respectively. From Eq. 4, the estimated residence time of the ion is about 0.01 ms.

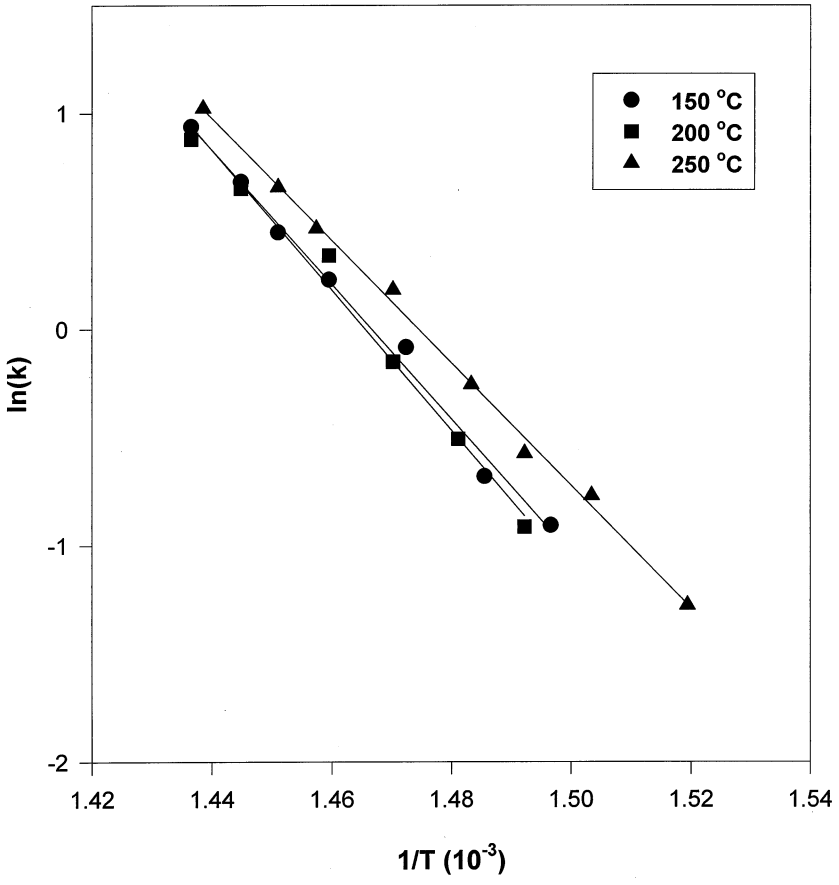

Fig. 6. Arrhenius plots of the data displayed in Fig. 4. Note that the lines are nearly parallel for the three temperatures of Segment1.

The Arrhenius plots of the data presented in Fig. 5, where three Segment1 temperatures are chosen, are shown in Fig. 6. The Arrhenius plots of the three temperatures are linear and nearly parallel. An average E_a(HCD) is obtained with a deviation corresponding to 2.65 ± 0.08 eV. Similarly, log A(HCD) values are also obtained that average to 25.5 ± 0.63.

The results are compared to those obtained using BIRD experiments on the same systems. Details of the BIRD results are available on a separate publication [30]. The values obtained from BIRD are tabulated together with HCD values in Table 1. A direct comparison of the two sets of values show that the E_a values from HCD experiments are consistently larger than the BIRD value by 1.5 eV. Log A shows the same consistent trend with the HCD values larger than the BIRD values by about 14.6 eV.

4. Discussion

The characterization of the dissociation process in a heated capillary tube is complicated by several processes. For further discussions on the general use of ESI to characterize noncovalent interactions the reader is referred to a review article by Smith [9]. We identify at least three sources that may contribute energy to the complex: the heated tube, the expansion from a relatively high pressure region of the tube to a low pressure region before the skimmer, and the

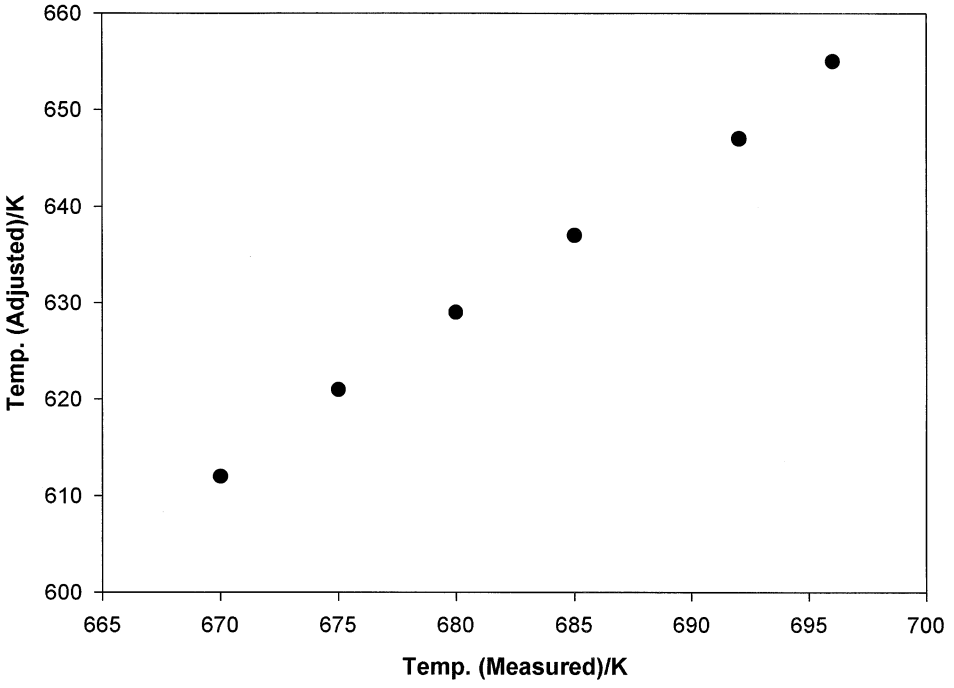

Fig. 7. Plot of $T_{\text{effective}}$ vs T_{measured}. $T_{\text{effective}}$ is obtained by assuming a constant difference in ln A and E_a.

collision induced dissociation because of the voltage differences between the capillary and the skimmer (also known as nozzle-skimmer dissociation).

The total internal energy (E_{total}) of the ion as it emerges the skimmer is given by:

$$E_{\text{total}} = E_{\text{thermal}} + E_{\text{expansion}} + E_{\text{CID}} \quad (5)$$

where E_{thermal} is the energy acquired in the heated capillary, $E_{\text{expansion}}$ is the energy acquired during the expansion, and E_{CID} is the energy acquired when the ion collides with neutrals between the capillary and the skimmer. Admittedly, this approach is rather simplistic as several other processes as may occur such as resolvation of the ion after the expansion followed by collision with neutrals to desolvate the ion again. Both E_{thermal} and E_{CID} increase the energy of the ion, while $E_{\text{expansion}}$ decreases it. The effect of E_{CID} on typical ESI spectra is readily observed. Nozzle-skimmer CID was used by Prokai et al. to dissociate complexes of amino acid and cyclodextrin [34]. On our instrument, varying this potential drop changed the Arrhenius parameters. For this reason, it was minimized as much as possible but still provided adequate signal for analysis. Even if the skimmer zone CID affects the outcome of the Arrhenius plot, it should lower the apparent E_a relative to BIRD. Instead, the E_a(HCD) values are found to be always higher than the E_a obtained by BIRD. We attempted to extrapolate the value of E_{CID} to zero energy, however this produced incoherent results. Because of the dynamic nature of the ionization source, the direct contribution of both $E_{\text{expansion}}$ and E_{CID} cannot be characterized without considerable effort.

It is believed that the uncertainty in the temperature measurement contributes the most to the discrepancy between HCD and BIRD values. An effective temperature can be calculated by assuming a constant difference in E_a and ln A between the BIRD and the HCD results. Fig. 7 shows the plot of the effective temperature ($T_{\text{effective}}$) versus the measured temperature (T_{measured}). Over the narrow temperature range ($\sim$ 30 K), the plot is linear with a slope of 1.6. The narrow range is limited by the BIRD results. It is expected that at a wider range, the plot will diverge

from linearity as shown by the temperature measurements of the outflow (Fig. 2). The average difference between T_{measured} and $T_{\text{effective}}$ is 49.5 K. The deviation of the slope away from unity prohibits the determination of E_a directly from HCD alone.

The determination of the temperature is a difficult problem that may diminish the utility of this method. Another problem is in defining a distinct temperature. As the tube is heated in the presence of the constant flow, a temperature gradient exist throughout the length of the capillary. As the ions traverse through the capillary it will experience a gradually increasing temperature. Furthermore, dissociation can occur all along the capillary at different temperatures. Lengthening the capillary to ensure equilibrium between the interior and the exterior of the capillary does not help define the temperature.

5. Conclusion

The systematic nature of the error, as shown by the nearly constant values of ΔE_a and $\Delta \log A$, suggests that for similar systems the HCD values may be directly comparable. However, the peptides represent only a small group and further studies are required to determine what chemical factors are important and vary ΔE_a.

Because of the difficulty in obtaining a "true" temperature, HCD may not be a reliable method for obtaining E_a. Instead, we propose that the dissociation temperature (or T_d) be an alternative method for obtaining relative strengths of interaction. The T_d is a relative measure of ΔG. By selecting a temperature corresponding to a relative intensity, we indirectly define a specific K [Eq. (6)]. T is varied until T_d is obtained which corresponds indirectly to a value of ΔG

$$\Delta G = -RT \ln K \tag{6}$$

The relationship between ΔG and T is simpler and is not as affected by the nonlinearity of the value T. The value E_a is obtained from a plot of intensity versus $1/T$ which is more strongly affected by the nonlinear relationship between interior and exterior temperature. For comparing relative stabilities of the complexes, T_d may be a more reliable index of comparison.

Finally, a differentially heated capillary allows us to differentiate gas-phase versus solution-phase dissociation process. In addition, we find that the performance of the differentially heated capillary is generally better than a single heated stage. Better reproducibility is obtained with the two stages in the determination of E_a(HCD), A(HCD), and T_d, under identical experimental conditions.

Acknowledgement

Funding provided by the National Science Foundation is gratefully acknowledged.

References

[1] K.J. Light-Wahl, D.L. Springer, B.E. Winger, C.G. Edmonds, I. Camp, D.G., B.D. Thrall, R.D. Smith, J. Am. Chem. Soc. 115 (1993) 803.
[2] V. Katta, B.T. Chait, J. Am. Chem. Soc. 113 (1991) 8534.
[3] B. Rosinke, K. Strupat, F. Hillenkamp, J. Rosenbusch, N. Dencher, U. Kruger, H.J. Galla, J. Mass Spectrom. 30 (1995) 1462.
[4] B.L. Schwartz, D.C. Gale, R.D. Smith, A. Chilkoti, P.S. Stayton, J. Mass Spectrom. 30 (1995) 1095.
[5] P. Juhasz, K. Biemann, Carbohydr. Res. 270 (1995) 131.
[6] R. Bakhtiar, R.A. Stearns, Rapid Commun. Mass Spectrom. 9 (1995) 240.
[7] Y.L. Hsieh, Y.T. Li, J.D. Henion, B. Ganem, Biol. Mass Spectrom. 23 (1994) 272.
[8] M. Jaquinod, N. Potier, K. Klarskov, J.M. Reymann, O. Sorokine, S. Kieffer, P. Barth, V. Andriantomanga, J.F. Biellmann, A. Vandorsselaer, Eur. J. Biochem. 218 (1993) 893.
[9] R.D. Smith, K.J. Light-Wahl, Biol. Mass Spectrom. 22 (1993) 493.
[10] M. Jaquinod, E. Leize, N. Potier, A.M. Albrecht, A. Shanzer, A. Vandorsselaer, Tetrahedron Lett. 34 (1993) 2771.
[11] R.D. Smith, K.J. Lightwahl, B.E. Winger, J.A. Loo, Org. Mass Spectrom. 27 (1992) 811.
[12] S.K. Chowdhury, V. Katta, B.T. Chait, Rapid Commun. Mass Spectrom. 4 (1990) 81.
[13] M. Busman, A.L. Rockwood, R.D. Smith, J. Phys. Chem. 96 (1992) 2397.
[14] A.L. Rockwood, M. Busman, H.R. Udseth, R.D. Smith, Rapid Commun. Mass Spectrom. 5 (1991) 582.
[15] M.M.-N. (Mautner), A.R. Dongré, A. Somogyi, V.H. Wysocki, Rapid Commun. Mass Spectrom. 9 (1995) 829.

[16] S.G. Penn, F. He, M.K. Green, C.B. Lebrilla, J. Am. Soc. Mass Spectrom. 8 (1997) 244.
[17] A. Rontoyianni, I.M. Mavridis, J. Inclusion Phenomena Molec. Recog. Chem. 18 (1994) 211.
[18] A. Rontoyianni, I.M. Mavridis, E. Hadjoudis, A.J.M. Duisenber, Carbohydr. Res. 252 (1994) 19.
[19] J. Szejtli, Cyclodextrins and Their Inclusion Complexes; Akadémiai Kiadó, Budapest, 1982, p. 296.
[20] J. Szejtli, Pharma. Tech. Inter. 3 (1991) 16.
[21] H. Hirai, Y. Shiraishi, H. Mihori, T. Kawamura, Poly. J. 27 (1995) 1064.
[22] S. Letellier, B. Maupas, J.P. Gramond, F. Guyon, P. Gareil, Anal. Chim. Acta 315 (1995) 357.
[23] P.P. Korkas, E. Weber, M. Czugler, G. Narayszabo, J. Chem. Soc.-Chem. Com. 21 (1995) 2229.
[24] J.B. Cunniff, P. Vouros, J. Am. Soc. Mass Spectrom. 6 (1995) 437.
[25] P. Camilleri, N.J. Haskins, A.P. New, M.R. Saunders, Rapid Commun. Mass Spectrom. 7 (1993) 949.
[26] A. Selva, E. Redenti, M. Pasini, P. Ventura, B. Casetta, J. Mass Spectrom. 30 (1995) 219.
[27] K. Uekama, T. Irie, Drug Investigation 2 (1990) 22 (suppl. 4).
[28] H.J. Schneider, T. Blatter, S. Simova, J. Am. Chem. Soc. 113 (1991) 1996.
[29] P.D. Schnier, W.D. Price, R.A. Jockusch, E.R. Williams, J. Am. Chem. Soc. 118 (1996) 7178.
[30] S.G. Penn, F. He, C.B. Lebrilla, J. Phys. Chem. (1998), in press.
[31] J.A. Carroll, S.G. Penn, S.T. Fannin, J. Wu, M.T. Cancilla, M.K. Green, C.B. Lebrilla, Anal. Chem. 68 (1996) 1798.
[32] E.E. Gard, M.K. Green, H. Warren, E.J.O. Camara, F. He, S.G. Penn, C.B. Lebrilla, Int. J. Mass Spectrom. Ion Processes 158 (1996) 115.
[33] W.L. McCabe, J.C. Smith, P. Harricott, Unit Operations of Chemical Engineering, McGraw-Hill, New York, 1985.
[34] R. Ramanathan, L. Prokai, J. Am. Soc. Mass Spectrom. 6 (1995) 866.